ISSN 1590-8844
International Journal of Mechanics and Control, Vol. 16, No. 01, 2015

AN UNDERACTUATED MECHANICAL HAND: THEORETICAL STUDIES AND PROTOTYPING

Vincenzo Niola   Francesco Penta   Cesare Rossi   Sergio Savino

Department of Industrial Engineering, University of Naples “Federico II”, Naples, Italy

ABSTRACT

In the present paper a model of an underactuated tendon driven mechanical hand is proposed. The aim of the activity was to study the possibility of realization of a mechanical hand five fingers, the movement of which is realized by the use of one only actuator. The mechanism is conceived as an hand prosthesis. The main particularity of the device essentially consist in that it is based on an adaptive scheme. In this way it is possible to obtain that the three phalanxes of each of the fingers adapt their rotation to the grasped object shape. This will be obtained by non-extendible tendons. So each finger will grasp the object surface independently on the configuration of the finger itself and independently on the configuration of the other fingers.

Keywords: Mechanical hand; Hand Prostesis; Underactuated mechanism.

1 INTRODUCTION

In the last decades, many devices for human prostheses were developed improving the life quality of a number of people.
It is well-known that human hand is one of the most complex and multi-functional organ; even if the thumb capability to rotate is neglected, the hand still has 15 d.o.f. or even 17 if some movements of the thumb are considered. The great progress in actuator miniaturization and in the control systems made it possible to design multi-finger and multi-phalanx grasping tools operated by several actuators; nevertheless, both the mechanical parts and the control are very complex, hence the cost is very high while the reliability is rather low. For these reasons underactuated multi-finger grasping devices moved by a single actuator were proposed. So, several multi-finger systems working likewise the human hand or human prostheses have been developed. Despite the progress in micro motors developing, in the grasping devices that use fingers, if the system’s dimensions are comparable to those of an human hand, it is rather difficult to operate each of the finger phalanxes by a (micro)motor, so the fingers are moved by tendons.

Contact author: Cesare Rossi [1]
[1]Email: cesare.rossi@unina.it

In Fig. 1 some examples are shown. In Fig. 1,a is reported a scheme [1] of a five finger hand moved by a single actuator; the auto-adaptabilily of the fingers to the shape of the grasped object is obtained by means of “sliding pulleys". In fig. 1,b is shown a study [2] in which the synergy concept was developed, based on the anatomic links of the human hand between muscle and tendons mostly as far as the coordination of the fingers is concerned (eigenpostures); this was obtained, essentially, by means of some pulleys fitted on the same shaft but having different diameters, as shown in figure 1,c. It must be told that the early prototypes reached the desired finger positions not very accurately; the behaviour of the device was then improved by means of further mechanical and control complexity, using a further actuator and a gear system.
In Fig.1,d is shown a model [3] widely inspired to the human body; most of the phalanxes joints have variable stiffness, allowing higher efforts and better adaptability. Since the hand is designed to be a part of a mechanical arm, the motors are located in the arm. The fingers are operated in antagonistic way by two motors for each d.o.f. and 38 motors, fitted in the forearm, were used; hence the device is not underactuated.
In Fig.1,e is reported a first prototype (see e.g. [4]) developed at the Scuola Superiore Sant'Anna (Pisa, Italy) having 16 d.o.f., operated by 4 motors, which was further developed in subsequent research activities, (see e.g [5,6,7,8]). Another Italian research team, born from the collaboration between the University of Pisa and the

Research Center "E.Piaggio", rather recently, developed the hand shown in fig 1,f, (see e.g. [9]). The device is operated by one actuator only, the joints are based on the Hillberry joint and the tendon are elastic.

In Fig.1,g the Multifunctional Hand Prosthesis is reported [10]. Fluid operated actuator are used, fed by a pump fitted in the metacarpal together with micro-valves controlled by a micro-controller.

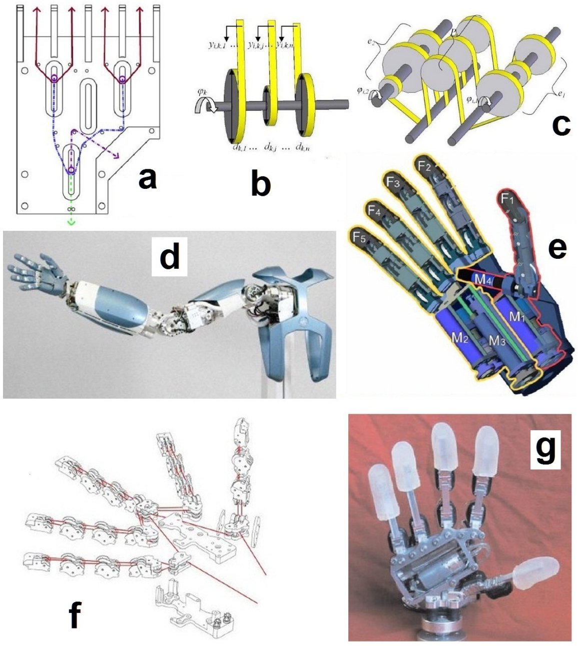

Figure 1 Examples of mechanical hands.

In Fig.2,a and b are reported the “Larm hand” and the kinematic scheme of one finger of a grasping device developed at the University of Cassino (Italy) [11,12,13,14], that essentially consists in a four finger underactuated hand.

In Fig.2,c is reported the Southampton Remedi Hand [15]; it has 6 d.o.f. with 6 small motors; 4 of them move the fingers and 2 move the thumb.

The above mentioned ones are perhaps among the most representative examples of mechanical hands. As for the underactuated designs, it must be sayd that they essentially belong to 2 types schematically shown in Fig.2,d. The soft synergy is essentially based on the presence of elastic tendons while the adaptive synergies is essentially based on differential mechanism. During the grasping, both the systems permit the fingers to adapt themselves to objects having a complicated shape (i.e. different sections in correspondence of each of the fingers), but the adaptive synergies with “rigid” tendons, permit, also, to grip the object exerting practically the same gripping force.

As for the tendon operated fingers, different solutions can be adopted as it was reported in [16]; essentially possible solutions range from a tendon for each of the phalanxes to a single tendon for the three phalanxes; the joints between the latter can be represented by simple hinges or more complex kinematic systems or even by simple elastic links.

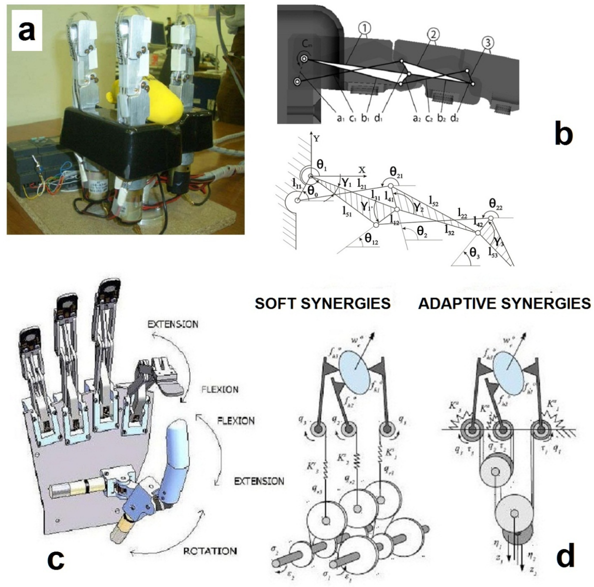

Figure 2 Examples of mechanical hands.

From the above reported, it seems interesting to study the possibility of designing a rather simple and cheap hand, based on adaptive synergies underactuated by means of a single actuator.

2 DESCRIPTION OF THE HAND

2.1 THE FINGER

Most of the choices adopted during the design phase of the device were based on the predictions of a hand model derived from the under-actuated finger mechanism presented in [18]. This mechanism is also shown in figure 3.

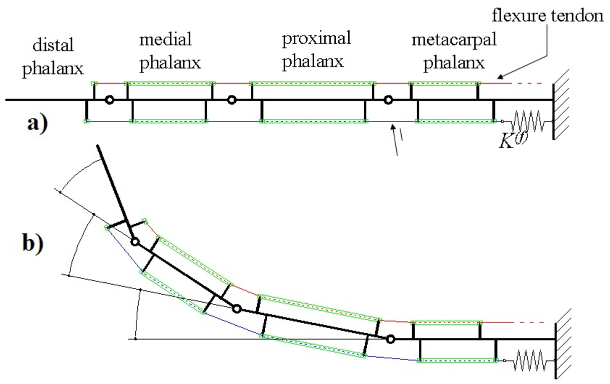

Figure 3 Scheme of the underactuated finger

It is a plane system having only three degrees of freedom, since it is composed of four rigid links connected together by three hinges free of friction. Of these four links, one is fixed and is indicated with the term metacarpal, the remaining three are movable and function as proximal, medial and distal phalanxes, respectively.

The finger is equipped with a flexural and an extensor tendon, both having an end fixed to the distal phalanx. The other end of the flexural tendon is mechanically linked to the differential mechanism, which transfers the hand actuator load (see sect. 2.2). The extensor tendon is instead elastically constrained to the metacarpus by a helical spring. All the phalanxes, furthermore, are provided with a couple of cylindrical guides along which the tendons can freely slide when the finger deforms. We assume that both the tendons are inextensible, free of thickness and have zero bending stiffness.

In the following, each finger of the hand device will be identified by a natural number *f*, with *f=1, 2, …, 5* and where *1* stands for the Thumb, *2* for the Index finger, …, *5* for the little finger, and a quantity pertaining to the finger *f* will be labeled by the superscript *f*.

As lagrangian coordinates of a finger we choose the absolute rotation $\varphi_1^{(f)}$ of its proximal phalanx, the relative rotation $\varphi_2^{(f)}$ between the proximal and the medial phalanx and, finally, the relative rotation $\varphi_3^{(f)}$ between the medial and the distal phalanx (fig. 3,b)).

Hence, denoting with $\boldsymbol{\varphi}^{(f)} = \left[\varphi_1^{(f)}, \varphi_2^{(f)}, \varphi_3^{(f)}\right]$ the column vector of the coordinates of the finger *f*, a hand configuration is univocally defined by the components of the column vector

$$\boldsymbol{\varphi} = \begin{bmatrix} \boldsymbol{\varphi}^{(1)} \\ \boldsymbol{\varphi}^{(2)} \\ \dots \\ \boldsymbol{\varphi}^{(5)} \end{bmatrix}.$$

In the present study the initial or reference configuration of the hand is the one with all the fingers totally extended (see fig. 3,a)), that is with all the rotations $\varphi_i^{(f)} = 0$.

For sake of simplicity, the hinges of a finger are numbered consistently with the adopted notation for the lagrangian coordinates: $i^{(f)}$ will denote the hinge where the rotation $\varphi_i^{(f)}$ occurs. Moreover, a movable phalanx is also identified by the same number of the hinge that is on its right side in the reference configuration.

In fig. 4,b) an enlarged view of the deformed configurations assumed by the extensor and flexure tendons close to the hinge $i^{(f)}$ is sketched.

Denoting respectively with $d_i^{(f)}$ and $s_i^{(f)}$ the fixed distances from the hinge centre of the points P_i and Q_i and with $\bar{d}_i^{(f)}$ and $\bar{s}_i^{(f)}$ those respectively of the points R_i and S_i, by the Carnot theorem, the following expressions for the lengths $\overline{P_iQ_i} = z_i^{(f)}$ and $\overline{R_iS_i} = l_i^{(f)}$ are obtained:

$$z_i^{(f)} = \sqrt{d_i^{(f)2} + s_i^{(f)2} - 2 \cdot d_i^{(f)} s_i^{(f)} \cos\left(\Phi_i^{(f)} - \varphi_i^{(f)}\right)}$$

$$l_i^{(f)} = \sqrt{\bar{d}_i^{(f)2} + \bar{s}_i^{(f)2} - 2 \cdot \bar{d}_i^{(f)} \bar{s}_i^{(f)} \cos\left(\bar{\Phi}_i^{(f)} + \varphi_i^{(f)}\right)},$$

where $\Phi_i^{(f)}$ and $\bar{\Phi}_i^{(f)}$ are the angles defined in fig. 4,a).

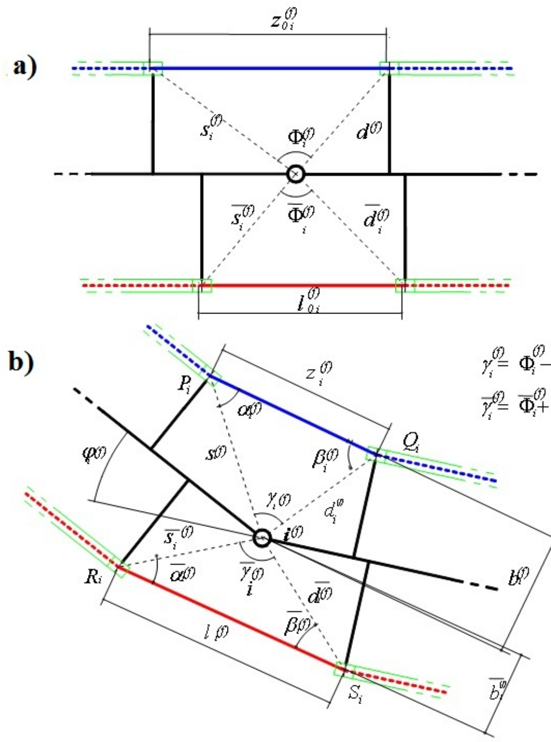

Figure 4 Inital (a) and deformed (b) configurations of the flexure and extensor tendons.

When the finger *f*, starting from the reference configuration, reaches the configuration $\boldsymbol{\varphi}^{(f)}$, the flexure tendon free paths $\overline{P_iQ_i}$ experience the shortenings

$$\Delta z_i^{(f)} = z_{0i}^{(f)} - z_i^{(f)},$$

with *i=1,…,3* and $z_{0i}^{(f)}$ initial value of $z_i^{(f)}$ (fig. 4,a)). Therefore, the end of the flexure tendon that is connected to the differential mechanism performs the displacement

$$u^{(f)} = \sum_{i=1}^{3} \Delta z_i^{(f)}.$$

Similarly, the free paths $\overline{R_iS_i}$ of the extensor tendon experience the length changes

$$\Delta l_i^{(f)} = l_i^{(f)} - l_{0i}^{(f)},$$

with $l_{0i}^{(f)}$ initial value of $l_i^{(f)}$. Therefore, the corresponding elongation of the spring connected to this tendon is:

$$\Delta l^{(f)} = \sum_{i=1}^{3} \Delta l_i^{(f)}.$$

In Fig 5 a simulation of the finger made by means of the multi -body code WM 2D™ is shown. In the figure the

ISSN 1590-8844
International Journal of Mechanics and Control, Vol. 16, No. 01, 2015

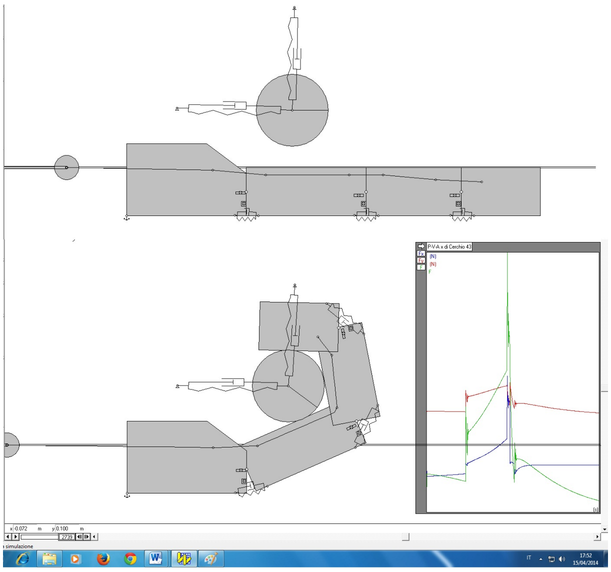

Figure 5 WM 2D™ model and simulations

grasping of an object is simulated; the object consists in a circle hold by two orthogonal elastic constraints. This simulates the self-adaptability of the underactuated finger to an object that moves or changes its shape during the grasping. From Fig.5 it is possible to observe that each of the three phalanxes correctly adapts its rotation to the object shape and to the object position respect to the finger itself. Moreover, in the same figure, the force in each of the elastic constraint (computed by the multi-body code) is also plotted; in this way the resultant of the grasping force can be also computed.

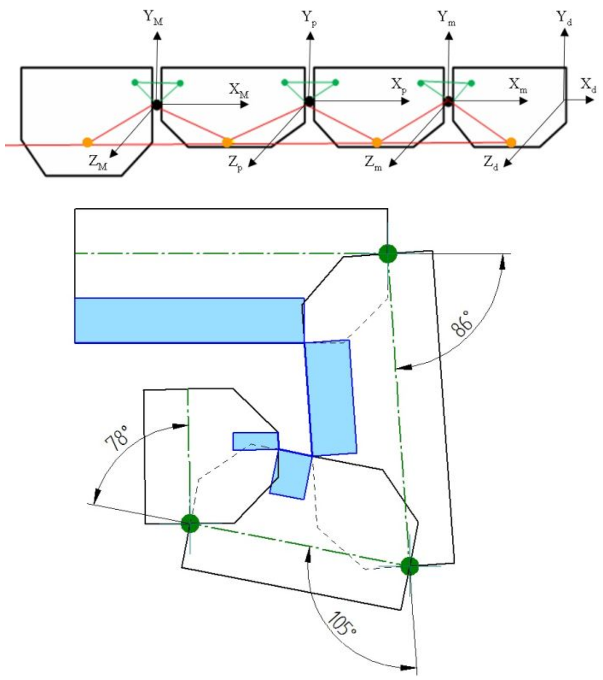

Figure 6 D-H representation and optimum computed domain of the tendon's guides.

Investigations were carried on in order to determine both the kinematic and the dynamic behavior of the underactuated finger [17, 18, 19, 20].
In particular, in fig. 6 the "Denavit and Hartemberg" representation of the finger model is represented together with the computed domain along the x and y axes of the tendon's guides.

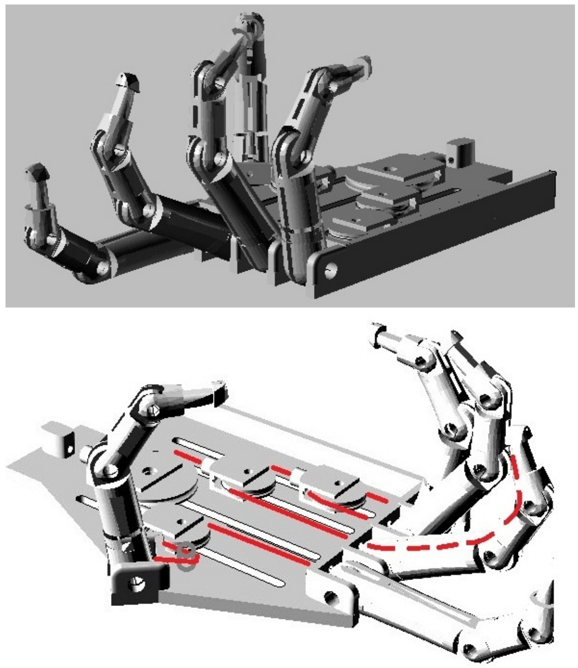

Figure 7 CAD design of the proposed device

2.1 THE HAND

In Fig. 7 CAD drawings of the first prototype of the hand are shown.
The hand was designed by using simple elements that guarantee the cheapness and simplicity of operation. In particular, the hand is composed by five fingers, each made of three phalanxes hinged to each other by pins, which represent the different articulations of a human finger. The finger is closed by means of an inelastic tie-rod as shown in Fig. 7.In the lower part of the figure one of the tendons inside the finger is represented with a dotted line; the tendons mechanism are also shown. Hence the working principle of the hand mechanism is evident.
In fig. 8 the scheme of the pulley system that permits the self-adapting of the fingers to the object shape during the grasping is shown together with the distribution of the force between the fingers of the hand. The repartition of the actuating force F allows to reach a configuration in which for each finger the force is:

F/4 on thumb;
F/4 on index;
F/4 on middle finger;
F/8 on ring finger;
F/8 on little finger.

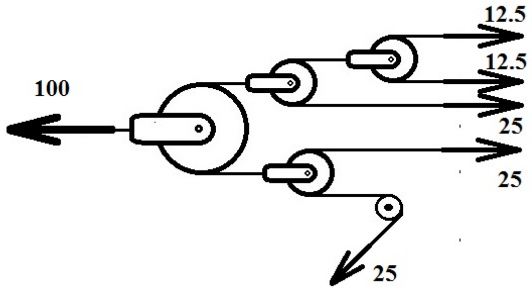

Figure 8 Pulleys system

The tendons, made of inelastic tie rod, passing through distribution pulleys system, distributes the gripping tension between the fingers. Thus permitting the fingers to adjust themselves to the grasped object size and shape.
The rotation of the pulleys, in fact, will occur at any contact of each phalanx with the gripped object. Once each phalanx enters into contact with the gripping object, the finger is aligned in such a way to tighten the object and ensure its grip. Thanks to the larger pulleys installed on the palm of the hand, the force is distributed also to the other fingers; the set will move up until each phalanx is in contact with the object to be taken, achieving the gripping.

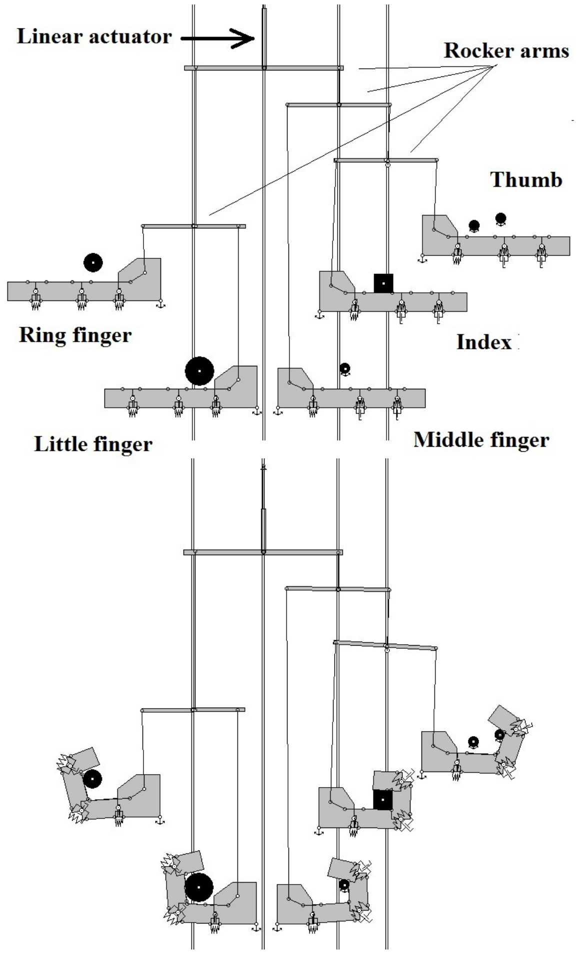

Figure 9 WM 2D™ model and simulations

The design of the hand was first studied by means of the multi-body code WM 2D™ again. In Fig. 9 the five finger model is shown. The model is essentially made by five fingers; each of them is almost equal to the one shown in Fig.3. The tendons are linked to the common linear actuator by means of rocker arm; each of the latter represents one of the pulleys of the pulley system. Since the rocker arms rotations are very little, the tendons kinematics does not differ significantly from the one of the pulley system.
In the upper part of Fig. 8 the hand is represented open, while in the lower part an object is grasped. The latter is represented in the simulation by means of the black fixed bodies; these represent the sections of the object in correspondence of each of the fingers. How it is possible to observe, in the shown simulation, the object section are very different in shape and position respect to the finger.
In the lower part of Fig. 9 the grasping is shown. How it can be observed, each of the fingers adapts its phalanxes rotation to the shape of the section the object presents to each of the fingers. This behavior is permitted because once a finger stops having touched the object, the rotation of a pulley (or of the rocker arm in the simulation) does not increase the tendon push but permits to the other tendons to move until the contact is reached by the other fingers. In other words, the pulley system permits that each of the non-extendible tendons is pulled always with the same amount of the actuator's force but its displacement is self-adapted to the phalanxes rotation required to grasp that section of the object.How it is possible to observe, despite the dynamical effects during the transient, the repartition of the forces is the one we had expected.
In fig. 10 an example of the simulation results is reported; the stress in the tendons during the grasping shown in fig.9. From the upper part of the figure the curves represent the thumb, the index, the middle and the ring finger, respectively. The curves have all the same magnification and are equally spaced along the vertical.

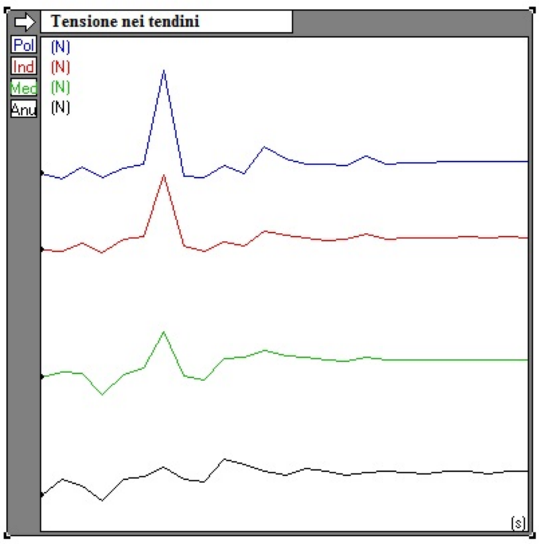

Figure 10 Example of the simulation results

2.1.1 Analisys of the grasping

We have analysed the hand behaviour during the grasping of an object fixed in the space. The analysis was conducted under the simplifying assumption that each finger initially touches the object with the proximal phalanx, then with the medial and finally with the distal one. Therefore, being the object fixed, when the phalanx $i^{(f)}$ is in contact with the object, only changes of the finger coordinates $\varphi_j^{(f)}$, with $j > i$, can occur (fig. 11).

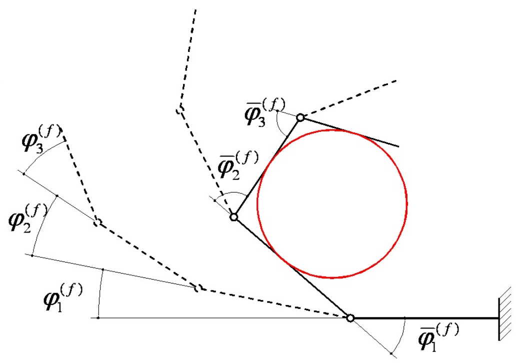

Figure 11 Deformed configurations of a finger during the grasping operation of an object.

If the hand actuator operates under displacement control during the grasping of the object, the hand equilibrium configurations $\boldsymbol{\varphi}$ have to satisfy both the stationary condition of the elastic strain energy E,

$$dE = d\left(\frac{1}{2}\sum_{f=1}^{5} K^{(f)} \Delta l^{(f)2}\right) =$$

$$= \sum_{f=1}^{5}\sum_{i=1}^{3} K^{(f)} \Delta l^{(f)} \cdot \frac{\partial \Delta l^{(f)}}{\partial \varphi_i^{(f)}} \cdot d\varphi_i^{(f)} = 0 \qquad \forall d\varphi_i^{(f)},$$

where $K^{(f)}$ is the stiffness of the spring connected to the extensor tendon of the finger f, the following constraint equation:

$$g(\boldsymbol{\varphi}) = u(\boldsymbol{\varphi}) - \bar{u} = 0$$

with $\bar{u}$ prescribed value for the displacement $u(\boldsymbol{\varphi})$ of the hand actuator, and the following contact conditions for the phalanxes touching the object:

$$\varphi_i^{(f)} - \bar{\varphi}_i^{(f)} = 0,$$

being $\bar{\varphi}_i^{(f)}$ the contact value of the coordinate $\varphi_i^{(f)}$, fig. 11.

According to the Lagrange multipliers method, the hand equilibrium problem is equivalent to searching for the stationary condition of the function:

$$\bar{E}_c = E(\boldsymbol{\varphi}) - \lambda \cdot g(\boldsymbol{\varphi}) - \sum_{(i,f)\in C} \mu_i^{(f)} \cdot \left(\varphi_i^{(f)} - \bar{\varphi}_i^{(f)}\right),$$

where the summation is extended to the set C of couples of index (i, f) identifying d.o.f.'s that are contact constrained. λ and $\mu_i^{(f)}$ are unknown Lagrange multipliers having respectively the meaning of load applied by the hand actuator to the differential mechanism and reaction moment with respect to the hinge i_f of the actions exerted by the object on the phalanxes j_f, with $j \geq i$.

The hand equilibrium equations, that are obtained by equating to zero the partial derivatives of the function $\bar{E}_c$, are non linear and have been solved numerically by the Newton-Raphson method following a small step incremental approach.

Some model predictions of the hand behaviour during both the free flexion of the fingers and the grasping of an object are synthetically presented in this section. The adopted values of the contact angles $\bar{\varphi}_i^{(f)}$ are listed in table I.

Table I - Contact angles $\bar{\varphi}_i^{(f)}$ (in degrees)

Finger	f	$\bar{\varphi}_1^{(f)}$	$\bar{\varphi}_2^{(f)}$	$\bar{\varphi}_3^{(f)}$
thumb	1	40°	68°	78°
index	2	35°	65°	70°
middle fin.	3	42°	70°	90°
ring finger	4	55°	81°	90°
little finger	5	70°	80°	90°

The numerical simulations have been carried out with an increment Δu of the actuator displacement u equal to 0.0125 mm. This value has been determined by trial and error and has proven be suitable to generate very small contact penetrations in each calculation step and to allow the Newton-Raphson algorithm to converge with very few iterations. Furthermore, checks for contact detection were carried out both at the beginning and at the end of each calculation step in order to detect changes of the contact conditions that may cause large penetrations in the subsequent step.

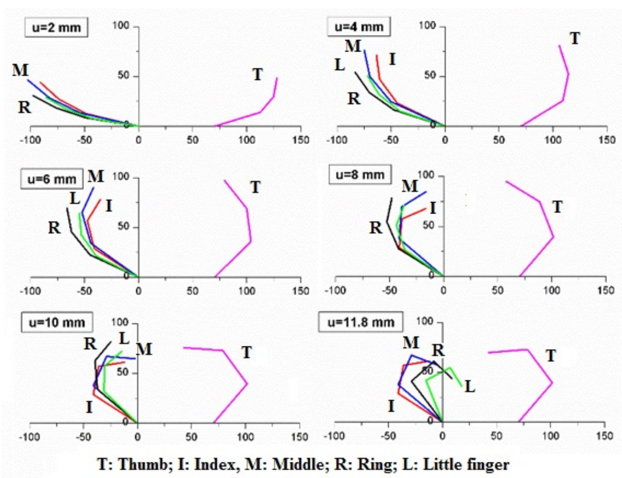

Figure 12 Deformed configurations of the fingers during the grasping of an object.

ISSN 1590-8844
International Journal of Mechanics and Control, Vol. 16, No. 01, 2015

In fig. 12 and fig. 13,a) are respectively shown the deformed configurations of the fingers for several values of the actuator displacement u and the diagram of the flexural tendons ends displacements $u_i^{(f)}$ as function of the actuator force λ. Inspection of these figures indicates that the geometry adopted for the fingers joints is such that, during the grasping operation, the relative rotations between phalanxes are always of the same sign, that is S-shaped configurations of the fingers does not occur. Furthermore, the displacements $u^{(f)}$ of each finger are continuous and increasing functions of the actuator force, since in the hand equilibrium paths are absent both snapping and buckling phenomena.

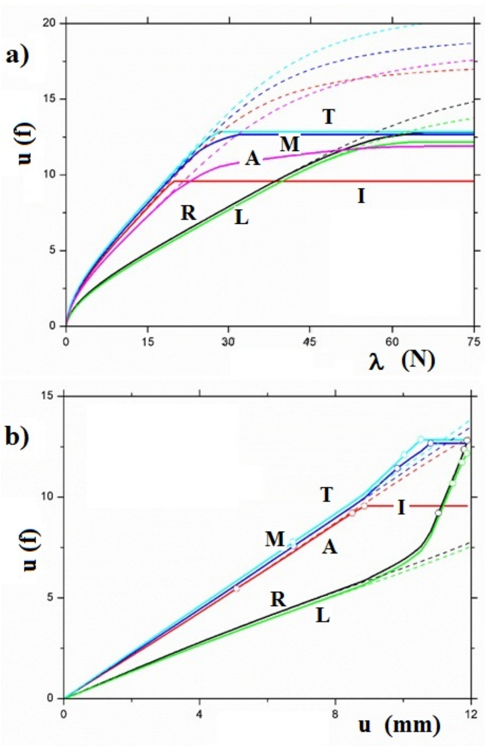

A: Actuator; T: Thumb; I: Index
M: Middle; R: Ring; L: Little finger

Figure 13 Diagram of the displacements $u^{(f)}$ of the flexural tendons ends as function of the actuator load λ, a), and of the actuator displacement u, b) (dash lines, free flexion of the fingers; solid lines, grasping action).

In the diagram of fig. 13,b) the displacements $u^{(f)}$ are plotted versus the actuator displacement u. Finger-object contact events are also marked by dot symbols along each curve.

By comparison with curves of fig. 13,a) and observing that the tractions in flexural tendons are proportional to the actuator force, the effects of the pulleys system of the differential mechanism are easily noted: the fingers stiffness changes due to contact events are totally compensated by the rotations of the pulley, without jumps in the tendon traction values. Thus, during the grasping operation, the values of the displacement increments imposed to the flexure tendons are continuously self-adapted to the actual finger contact conditions.

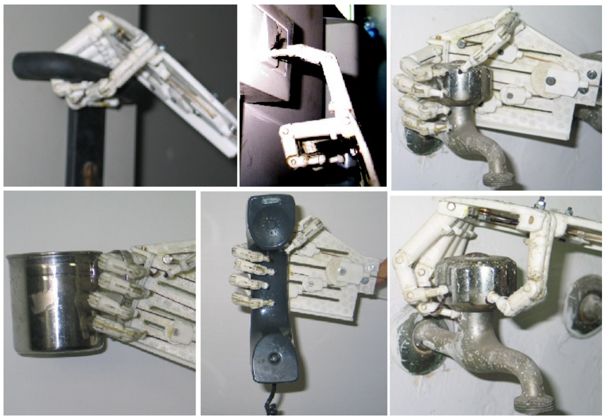

Figure 14 Examples of grasping of the first prototype

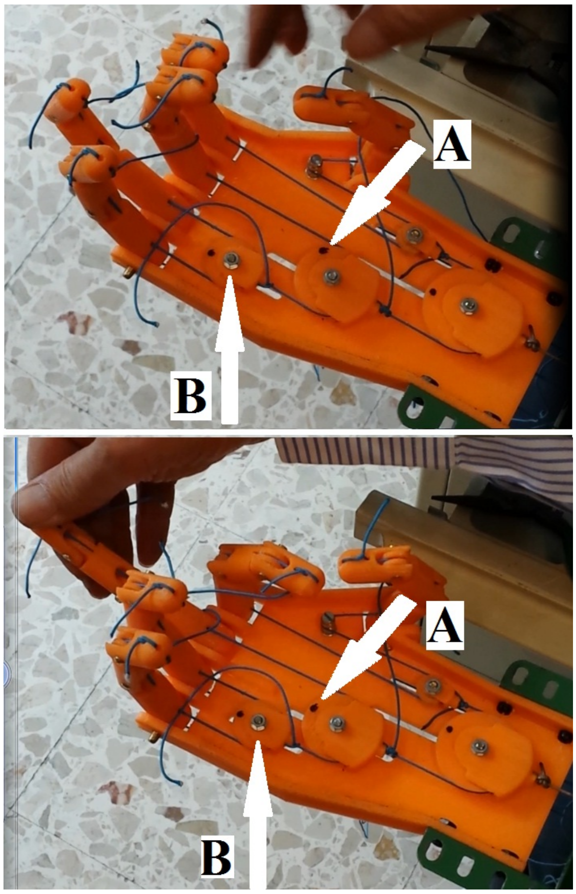

Figure 15 The second prototype.

3 THE PROTOTYPE

Two prototypes were built. In the first one the extension tendons were represented by simple rubber elastic bands.

In Fig. 14 examples of grasping of the first prototype are reported.

The second prototype was fitted with unextendible tendons, each connecter to a spring. In the figures 15 and 16 pictures of the second prototype are shown.

In Fig. 15 is shown how the three phalanxes of each of the fingers adapt their rotation: in both the figure the actuator was in the same position while the human hand forces a finger to move. By comparing the two images, it can be observed that when the middle finger is stretched, all the other fingers move; in particular, in this case, this movement is mainly permitted by the rotation of the pulley indicated by the arrow A (see the little mark on the pulley) and the translation of the pulley indicated by the arrow B.

In figure 16 the grasping of a rather complex object is shown. The object used for the reported grasping test is made by three different cylinders having rather different diamenters.

In the upper part of Fig. 16 the hand with the fingers completely released is shown while in the lower part the fingers are completely clamped on the object. How it is possible to observe, all the phalanxes automatically rotate in order to fall onto contact with the object surface, ensuring a satisfactory and stable grasping.

Both the prototypes wwere almost completely made by a 3D printer in polyactide (PLA), a thermoplastic aliphatic polyester, starting from the CAD drawings

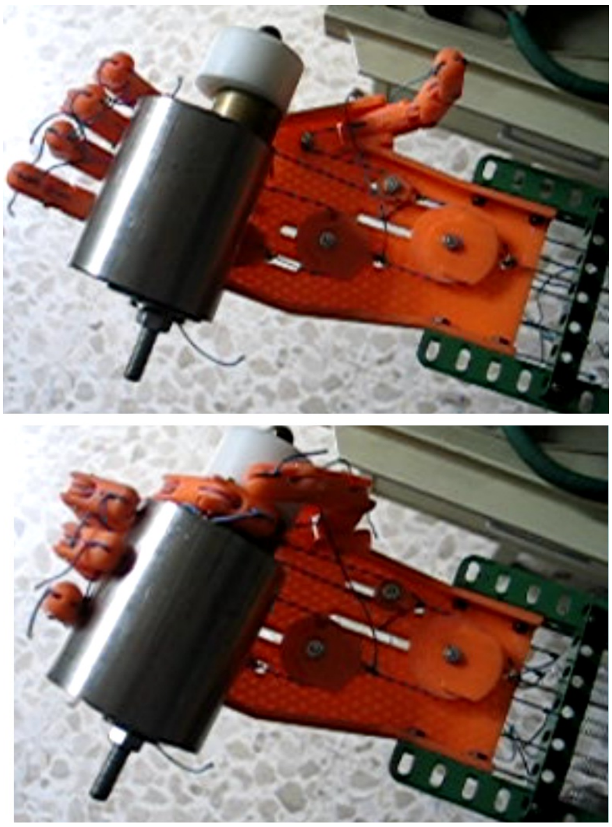

Figure 16 Grasping

4 CONCLUSIONS

Studies on kinematics and dynamics of an underactuated mechanical hand (presented in previous papers) permitted to design and built a first prototype that was the mail goal of this contribution; it has shown very encouraging results.

In conclusion the pulley system satisfactory works and shows a satisfactory auto-adaptability of the so actuated fingers, hence permitting to replicate several functions of a human hand.

REFERENCES

[1] Gosselin C., Pelletier F., Laliberte T. (2008) An Anthropomorphic Underactuated Robotic Hand with 15 Dofs and a Single Actuator. 2008 IEEE Int. Conf. on Robotics and Automation Pasadena, CA, USA, May 19-23, 2008.

[2] Brown C.Y., Asada H.H. (2007) Inter-Finger Coordination and Postural Synergies in Robot Hands via Mechanical Implementation of Principal Components Analysis. 2007 IEEE/RSJ Int. Conf. on Intelligent Robots and Systems San Diego, CA, USA, Oct 29 - Nov 2, 2007.

[3] Grebenstein M., Chalon M., Hirzinger G., and Siegwart R. (2010) Antagonistically Driven Finger Design for the Anthropomorphic DLR Hand Arm System. IEEE-RAS International Conference on Humanoid Robots Nashville, TN, USA, December 6-8, 2010.

[4] Controzzi M., Cipriani C. and Carrozza M.C. (2008) Mechatronic Design of aTransradial Cybernetic Hand. IROS February 22, 2008.

[5] Cipriani C., Controzzi M., Carrozza M. C., (2011) The Smart Hand Transradial Prosthesis, Journal Of Neuro-engineering And Rehabilitation, 2011, n. 8.

[6] Roccella S., Carrozza M.C., Cappiello G., Dario P., Cabibihan J.J., Zecca M., Miwa H., Itoh K., Matsumoto M., Takanishi A., Design, fabrication and preliminary results of a Novel anthropomorphic hand for humanoid robotics: RCH- 1, Proceedings of 2004 IEEE/RSJ International Conference on Intelligent Robots and Systems, Sendai, Japan, September 28 - October 2, 2004.

[7] S. Roccella, M.C. Carrozza, G. Cappiello, J.J. Cabibihan, C. Laschi, P. Dario, H. Takanobu, M. Matsumoto, H. Miwa, K. Itoh, A. Takanishi, Design and Development of Five-Fingered Hands for a Humanoid Emotion Expression Robot, International Journal Of Humanoid Robotics, 2007, n. 4, pp. 181-206.

[8] S. Roccella, E. Cattin, N. Vitiello, F. Giovacchini, A. Chiri, F. Vecchi, M.C. Carrozza, Design of a hand exoskeleton (handexos) for the rehabilitation of the hand, Gerontechnology; N. 7(2), 2008, pp. 197-197.

[9] M.G.Catalano, G.Grioli, A.Serio, E.Farnioli, C.Piazza, A.Bicchi (2012) Adaptive Synergies for a Humanoid Robot Hand. Proc. of IEEE-RAS

International Conference on Humanoid Robots Osaka, Japan, Nov. 29th - Dec. 1st, 2012.

[10] C.Pylatiuk, S.Mounier, A.Kargov, S.Schulz, G.Bretthauer (2004) Progress in the Development of a Multifunctional Hand Prosthesis. Proc. of the 26th Annual International Conf. of the IEEE EMBS San Francisco, CA, USA, September 1-5, 2004.

[11] Carbone G. and Ceccarelli M. (2008) 'Experimental Tests on Feasible Operation of a Finger Mechanism in the LARM Hand ', Mechanics Based Design of Structures and Machines, 36:1, pp. 1 – 13, doi: 10.1080/15397730701729445

[12] Wu Li Cheng, Carbone G., and Ceccarelli M. (2009) 'Designing an underactuated mechanism for a 1 active DOF finger operation' Mechanism and Machine Theory 44, 2009, pp. 336–348.

[13] Carbone G., Ceccarelli M. (2008) 'Design of LARM Hand: Problems and Solutions' Journal of Control Engineering and Applied Informatics, Vol.10, n.2, pp. 39-46.

[14] Yao S., Ceccarelli M., Carbone G., Zhan Q. and Lu Z. (2011) 'Analysis and optimal design of an underactuated finger mechanism for LARM hand' Front. Mech. Eng. 2011, 6(3), pp. 332–343, doi: 10.1007/s11465-011-0229-8

[15] D.P.J. Cotton, A. Cranny, P.H. Chappell, N.M. White, S.P. Beeby, Control Strategies For A Multiple Degree Of Freedom Prosthetic Hand. Electronic Systems Design Group, School of Electronics and Computer Science, University of Southampton, 2006.

[16] F. Lotti, G. Vassura (2012) Sviluppo Di Soluzioni Innovative Per La Struttura Meccanica Di Dita Articolate Per Mani Robotiche. Associazione Italiana per l'Analisi delle Sollecitazioni (AIAS) XXXI Convegno Nazionale, 18-21 September 2002, Parma.

[17] Fiore P., Niola V., Pisani G., Rossi C., Savino S., Troncone S., "A model of a robotic hand based on a tendon driven mechanism", Proc. of 22th Internation Workshop on Robotics in Alpe-Adria-Danube Region, Portorož, Slovenia, September 11-13, 2013.

[18] Rossi C., Savino S., "Mechanical Model of a Single Tendon Finger", Proc. of ICNAAM 2013: 11th International Conference of Numerical Analysis and Applied Mathematics, Rhodes, Greece, Sep 21-27, 2013.

[19] Rossi C., Savino S, "An underactuated multi-finger grasping device", International Journal of Advanced Robotic Systems, Vol. 11(1), 17 February 2014, Article number 20.

[20] Rossi C., Savino S., Niola V., Troncone S., "A Study of a Robotic Hand with Tendon Driven Fingers", Robotica. ISSN: 0263-5747, doi: 10.1017/S02635 74714001179.

[21] F. Penta, C. Rossi, S. Savino, An Underactuated Finger for a Robotic Hand, International Journal of Mechanics and Control, Vol. 15(2), 2014, ISSN: 1590-8844.